First-principles thermodynamics of La2O3-P2O5 pseudobinary system

Toyoura, Kazuaki; Hatada, Naoyuki; Nose, Yoshitaro; Uda, Tetsuya; Tanaka, Isao

PHYSICAL REVIEW B **84**, 184301 (2011)

First-principles thermodynamics of La_2O_3-P_2O_5 pseudobinary system

Kazuaki Toyoura,[1,*] Naoyuki Hatada,[1] Yoshitaro Nose,[1] Tetsuya Uda,[1] and Isao Tanaka[1,2]
[1]*Department of Materials Science and Engineering, Kyoto University, Yoshida, Sakyo, Kyoto 606-8501, Japan*
[2]*Nanostructure Research Laboratory, Japan Fine Ceramics Center, Atsuta Nagoya 456-8587, Japan*
(Received 26 July 2011; revised manuscript received 23 September 2011; published 14 November 2011)

Phase stabilities in the La_2O_3-P_2O_5 pseudobinary system have been theoretically analyzed. Phonon modes of five crystals, i.e., La_2O_3, La_3PO_7, $LaPO_4$, LaP_3O_9, and LaP_5O_{14}, and vibrational modes of gaseous P_2O_5(g) are computed from first principles in order to obtain the contribution of vibrations to the free energy. Additional dynamical contributions, i.e., rotations and translations are also taken into account for the gaseous P_2O_5(g). Vibrational states strongly reflect the crystal structures and bonding states. In this system, the strong P-O covalent bonds in PO_4 units and the relatively weak La-O bonds are found to be the key factors determining the vibrational spectra. In the oxyphosphate, La_3PO_7, the two bonding states are coexisting, and the vibrational spectrum is approximately an average of La_2O_3 and $LaPO_4$. On the other hand, the P_2O_5-rich compounds, i.e., LaP_3O_9 and LaP_5O_{14}, cannot be treated in the same manner. Their PO_4 units form corner-sharing networks whose vibrations are strongly correlated. The networks raise the vibrational frequencies, leading to high-frequency modes up to 40 THz. The Gibbs energies using the calculated vibrational spectra are in reasonable agreement with the available data of La_2O_3, $LaPO_4$, and P_2O_5(g), e.g., the differences between the calculated and reported values are less than 2 kJ/mol-atom (20 meV/atom) at 1500 K. The Gibbs energies and the phase stabilities of the other three compounds, La_3PO_7, LaP_3O_9, and LaP_5O_{14}, are evaluated, whose data are yet unknown so far.

DOI: 10.1103/PhysRevB.84.184301 PACS number(s): 63.70.+h

I. INTRODUCTION

Lanthanide phosphates have received much attention due to their various potential applications such as catalysts, phosphors, and proton conductors.[1–3] They have been synthesized by many different routes. However, the most important data necessary for rational processing are lacking: Thermodynamic data and equilibrium phase diagrams,[4,5] which can provide information on phase stabilities and process routes, have not been well established in most of lanthanide phosphate systems.

In the La_2O_3-P_2O_5 system, two phase diagrams have been reported,[6,7] in which seven intermediate compounds were suggested, i.e., La_5PO_{10}, La_3PO_7, $La_7P_3O_{18}$, $LaPO_4$, $La_2P_4O_{13}$, LaP_3O_9, and LaP_5O_{14}. As for their thermodynamic properties, the standard enthalpies, entropies, and Gibbs energies of formation and the standard entropies at 298 K ($\Delta H^\circ_{f,298\,\mathrm{K}}$, $\Delta S^\circ_{f,298\,\mathrm{K}}$, $\Delta G^\circ_{f,298\,\mathrm{K}}$, and $S^\circ_{298\,\mathrm{K}}$ are available only for $LaPO_4$.[8–14] But, the reported values are widely scattered, e.g., $\Delta G^\circ_{f,298\,\mathrm{K}}$ is in the range of 200 kJ/mol.

For discussion of their phase stabilities, phonon modes are computed from first principles in order to obtain the contribution of vibrations to the free energy. Additional dynamical contributions, i.e., rotations and translations are taken into account for a gas phase. Vibrational spectra strongly reflect the crystal structures and bonding states. In this system, the crystal structures of lanthanum phosphates except oxyphosphates are composed of La^{3+} cations and PO_4^{3-} anions. It is widely accepted that the P-O covalent bonds in the PO_4 units are strong, leading to high-frequency phonon modes. Although the presence of the high-frequency modes has been observed in experimental Raman and infrared spectra,[15] first-principles phonon calculations of lanthanide phosphates have not been reported to the authors' knowledge. The neighboring PO_4 tetrahedra are corner shared to form the infinite networks in LaP_3O_9 and LaP_5O_{14}, which can also bring changes to the vibrational states. In the case of oxyphosphates, oxygen atoms form La-O bonds similar to those in La_2O_3, in addition to the P-O covalent bonds in PO_4 units. In the present study, the vibrational spectra are discussed from the viewpoints of the crystal structures and bonding states.

Using the calculated vibrational spectra, the Gibbs energies are evaluated as a function of temperature. Solid phases subjected to the analysis are La_2O_3, La_3PO_7, $LaPO_4$, LaP_3O_9 and LaP_5O_{14}, in which information of the crystal structure is available. A gas phase, P_2O_5(g), is also examined, taking the rotational and translational contributions to the Gibbs energy into account. Here the conventional expression of "P_2O_5 gas" is used, although it consists of P_4O_{10} molecules. The suffix (g) denotes a gas phase. No suffix is used for a crystalline phase.

II. METHODOLOGY

A. Gibbs energies of solid and gas phases

Phase stabilities can be discussed using Gibbs energies, $G = U + PV - TS$, where U is the internal energy, P is the pressure, V is the volume, T is the temperature, and S is the entropy. In the case of solid phases under atmospheric pressure, Gibbs energies can be approximated by Helmholtz energies, F, since the PV term is negligible. Lattice vibrations are the major contribution to the temperature dependences of Helmholtz energies of solid phases. It can be given by the summation of the static energies without lattice vibrations, E_{stat}, and the vibrational free energies, F_{vib}, as follows:

$$G_{\mathrm{solid}} \simeq E_{\mathrm{stat}} + F_{\mathrm{vib}}. \quad (1)$$

In the case of gas phases, the rotational free energies, F_{rot}, and the translational free energies including the PV term, G_{trans}, also have contributions to the Gibbs energies in addition to the static energies and the vibrational free

TABLE I. Calculated lattice parameters of La_2O_3, La_3PO_7, $LaPO_4$, LaP_3O_9, and LaP_5O_{14}. The experimental values used as the initial structures are also shown for reference.

	Space group		Lattice parameters			
			a	b	c	β
La_2O_3	$P3m1$	Calc. (this work)	3.94		6.18	
		Expt.[a]	3.94		6.13	
La_3PO_7	Cm	Calc. (this work)	13.26	13.71	12.51	108.6
		Expt.[b]	13.09	13.59	12.43	110.0
$LaPO_4$	$P12_1/n1$	Calc. (this work)	6.80	7.04	6.48	103.3
		Expt.[c]	6.831	7.071	6.503	103.3
LaP_3O_9	$C222_1$	Calc. (this work)	11.41	8.74	7.49	
		Expt.[d]	11.30	8.65	7.40	
LaP_5O_{14}	$P12_1/c1$	Calc. (this work)	8.94	9.30	13.28	90.32
		Expt.[e]	8.821	9.120	13.171	90.66

[a]Reference 25.
[b]Reference 26.
[c]Reference 27.
[d]Reference 28.
[e]Reference 29.

energies:

$$G_{\text{gas}} \simeq E_{\text{stat}} + F_{\text{vib}} + F_{\text{rot}} + G_{\text{trans}}. \quad (2)$$

In the present study, the lattice and molecular vibrations were treated under the harmonic approximation. The static energies are directly obtained as the total energies at 0 K by the electronic structure calculations, and the vibrational free energies are given by

$$F_{\text{vib}} = \sum_i \left\{ \frac{1}{2} h\nu_i + kT \ln\left(1 - \exp\left(-\frac{h\nu_i}{kT}\right)\right)\right\}, \quad (3)$$

where ν_i is the vibrational frequency of the i-th normal mode, h is the Planck constant, and k is the Boltzmann constant. Molecular rotations were treated as a rigid rotor to evaluate the rotational free energies of gases. The energy levels are expressed as $BJ(J+1)$ $(J = 0, 1, \ldots)$, where B is the rotational constant related to the moment of inertia of molecules. The symmetry number of P_4O_{10} molecule was taken into consideration in estimation of the rotational free energy. Using the ideal gas approximation, the translational free energies are given by $kT\ln(pV_Q/kT)$ on the basis of quantum mechanics. V_Q is the quantum volume defined as $(h^2/2\pi mkT)^{3/2}$, where m is the mass of molecules.

B. Computational conditions

All the calculations were performed from first principles using the projector-augmented wave (PAW) method[16] implemented in the VASP code.[17–21] The generalized-gradient approximation (GGA-PBE) parameterized by Perdew, Burke, and Ernzerhof[22] was used for the exchange-correlation term. The plane-wave cutoff energy was 400 eV. The $5s$, $5p$, $6s$, and $5d$, orbitals for lanthanum, $3s$ and $3p$ for phosphorus, and $2s$ and $2p$ for oxygen were treated as valence states. The supercells employed in the present study were $3 \times 3 \times 2$ unit cells for La_2O_3, $2 \times 2 \times 2$ for $LaPO_4$ and LaP_3O_9, $2 \times 2 \times 1$ for LaP_5O_{14}, and $1 \times 1 \times 1$ for La_3PO_7. The k-point meshes were $2 \times 2 \times 2$ meshes for La_3PO_7, LaP_3O_9, and LaP_5O_{14}, and $1 \times 1 \times 1$ for La_2O_3 and $LaPO_4$. Atomic positions were

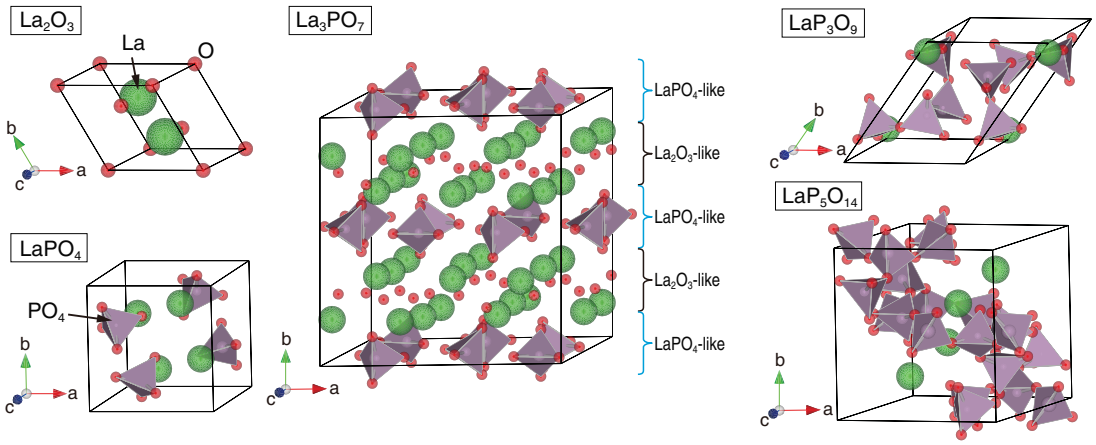

FIG. 1. (Color online) Crystal structures of La_2O_3, La_3PO_7, $LaPO_4$, LaP_3O_9, and LaP_5O_{14}. The red (small) and green (large) balls denote La and O, and the purple tetrahedra denote PO_4 units. La_3PO_7 has a stacked structure of La_2O_3-like and $LaPO_4$-like structures.

fully optimized until the residual forces become less than 1×10^{-5} eV/Å, since phonon calculations are sensitive to the residual forces of the structures before displacements.[23,24] Phonon calculations were made by the direct method using the phonopy code.[24] Each atom in the supercells was displaced by ±0.01 Å in each of x, y, and z directions to obtain all the interatomic force constants.

III. RESULTS AND DISCUSSION

A. Crystal structures and static energies

Experimental crystal structures in the La_2O_3-P_2O_5 system are known for La_2O_3, $LaPO_4$, LaP_3O_9, and LaP_5O_{14}.[25–29] As for La_3PO_7, only the space group, Cm, and the cell parameters were reported.[30] The fractional coordinates of an isostructural compound, Nd_3PO_7, were used as initial inputs for the structural optimization of La_3PO_7. Table I summarizes the theoretical and experimental lattice parameters of each solid phase. The differences between the theoretical and the experimental values are less than 2%. Figure 1 shows the crystal structure of each phase. Neighboring PO_4 tetrahedra are corner shared in LaP_3O_9 and LaP_5O_{14} to form PO_4 infinite networks, while all the tetrahedra are isolated in $LaPO_4$. The crystal structure of La_3PO_7 can be considered as a stacked structure of La_2O_3-like and $LaPO_4$-like layers. It is interesting that the two bonding states, P-O and La-O bonding, are coexistent in the oxyphosphate, which leads to the notable vibrational spectra as described in the following subsection.

Figure 2 shows the calculated static energy of each phase with reference to the static energy of the mixture of La_2O_3 and P_2O_5(g) at the corresponding ratio of x, which is called the mixing static energy in this paper. The polygonal line connecting all the points shows a convex hull, which means all the compounds do not decompose into the neighboring phases from the viewpoint of the static energies.

B. Vibrational density of states

Figure 3 shows the total and partial vibrational density of states of each phase computed in the present study. The black lines denote the total density of states, and the green, blue, orange, and red lines are contributions of lanthanum, phosphorous, oxygen with La-O bonds, and oxygen with P-O bonds, respectively. The regions below 0 THz correspond to imaginary frequencies. Tiny imaginary frequencies appear in a few compounds. Detailed inspection of their phonon dispersion curves found that the imaginary modes do not appear at wave vectors that are commensurate with the periodicity of the supercell. The imaginary modes can therefore be attributed to numerical errors. The neglect of the imaginary modes does not increase the error of our free energy estimation, e.g., <1 kJ/mol-atom (<0.01 eV/atom) at 1500 K.

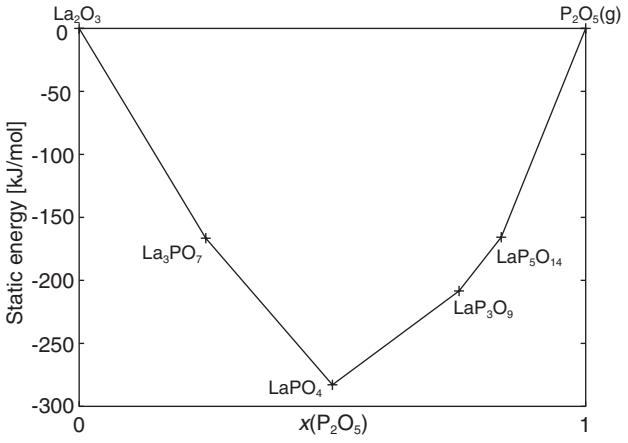

FIG. 2. Calculated static energy of each phase in the La_2O_3-P_2O_5 system. The energy reference is the static energy of the mixture of La_2O_3 and P_2O_5(g) in each ratio of x.

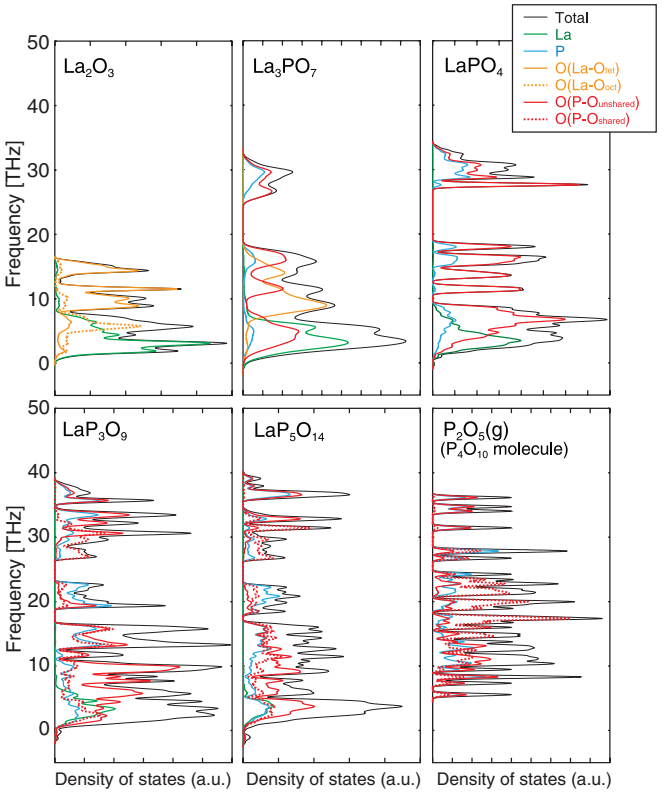

FIG. 3. (Color online) Total and partial density of states for lattice vibrations of each phase in the La_2O_3-P_2O_5(g) system. The black lines denote the total density of states, and the green (light gray), blue (gray), orange (medium gray), and red (dark gray) lines are contributions of lanthanum, phosphorous, oxygen with La-O bonds, and oxygen with P-O bonds, respectively. The O contribution with P-O bonds is subdivided into two, i.e., corner shared and unshared by PO_4 tetrahedra, shown by the solid and dotted lines, respectively. Oxygen atoms with La-O bonds are also distinguished by the coordination number, 4 and 6, by the solid and dotted lines. The regions below 0 THz correspond to imaginary frequencies.

The eigenfrequencies of the La contribution are relatively low in all the compounds due to the heavy La nucleus, which is located mainly below 10 THz. In contrast, the P contribution has higher frequencies, reflecting the strong covalent bonding between P and O. The contributions of P and O with P-O covalent bonds, i.e., the PO_4 contribution, can be classified into three types. The first type is vibrations without deformation of PO_4 units, having low frequencies less than 10 THz. The second has middle frequencies in the range of 10 THz to 25 THz, corresponding to PO_4 bending modes with the O-P-O

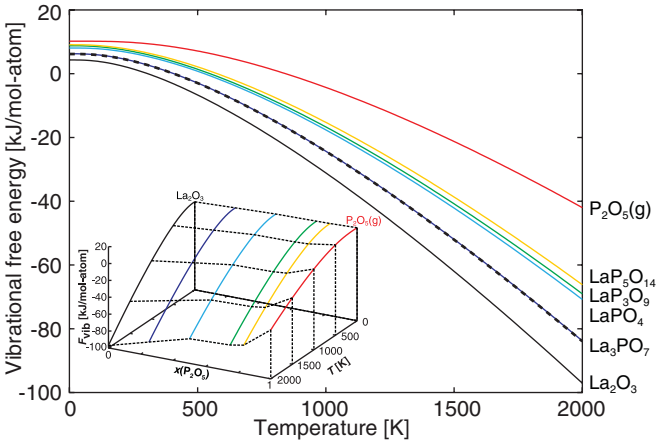

FIG. 4. (Color online) Vibrational free energies of La_2O_3, La_3PO_7, $LaPO_4$, LaP_3O_9, LaP_5O_{14}, and P_2O_5(g) as a function of temperature. The broken line denotes the average vibrational free energy of La_2O_3 and $LaPO_4$.

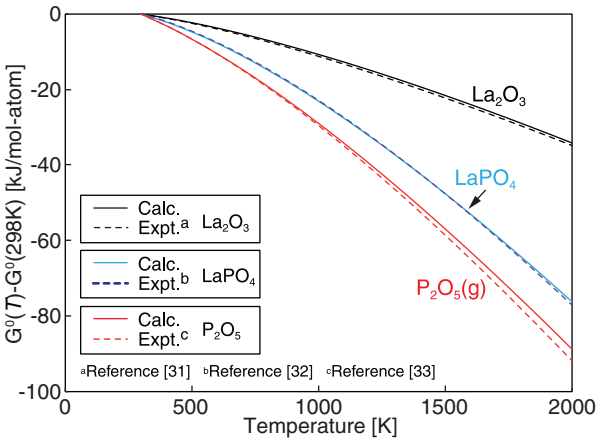

FIG. 6. (Color online) The standard Gibbs energies of La_2O_3 (black [top] lines), $LaPO_4$ (blue [middle] lines), and P_2O_5(g) (red [low] lines) with reference to those at 298 K. The solid and broken lines denote the calculated and experimental values, respectively.

angles changed. The third is attributed to PO_4 stretching with change in length of P-O bonds, having high frequencies of more than 25 THz. In the P_2O_5-rich compounds, LaP_3O_9 and LaP_5O_{14}, neighboring PO_4 tetrahedra are corner shared to form infinite PO_4 networks. Their vibrational states are different from $LaPO_4$ that includes only isolated PO_4 units. Remarkably, LaP_3O_9 and LaP_5O_{14} have higher-frequency modes close to 40 THz, which do not exist in $LaPO_4$. The vibrational modes are attributed to stretching of the P-O bonds with the corner-shared oxygen atoms, which are strongly pinned at the original positions. The PO_4 vibrations are thus strongly correlated through the corner-shared oxygen atoms, leading to the rise of the vibrational frequencies in the two phosphates.

On the other hand, the O contribution with La-O bonds shows relatively low frequencies less than 18 THz. The oxyphosphate, La_3PO_7, is interesting in terms of the coexisting of the two kinds of oxygen atoms with P-O and La-O bonds. The vibrational spectra can be approximated as the average of La_2O_3 and $LaPO_4$, reflecting the stacked structure of the two phases. The discrepancy between the averaged and calculated spectra of La_3PO_7 is derived from the coupling between the La_2O_3-like and $LaPO_4$-like layers. Particularly, some of the bending modes of PO_4 tetrahedra in the $LaPO_4$-like layers are strongly coupled with the vibrations of oxygen atoms in the La_2O_3-like layers. The coupling leads to the large difference in the contribution of oxygen atoms with P-O bonds between $LaPO_4$ and La_3PO_7, in the range of 10 THz to 18 THz. In addition, the difference in La-O bonding states also creates a difference between the averaged and calculated spectra. Oxygen atoms in La_2O_3 are classified into two, i.e., tetrahedrally and octahedrally coordinated ones by lanthanum atoms, O_{tet} and O_{oct}, respectively. Meanwhile only O_{tet} exists in the La_2O_3-like layers of La_3PO_7. The O_{oct} contribution has a large peak at around 6 THz, which is located in the lower-frequency region than that of the O_{tet} contribution.

The vibrational spectra are related to the crystal structures and bonding states in this way. The strong P-O bonds forming PO_4 tetrahedra are the origin of the high-frequency modes,

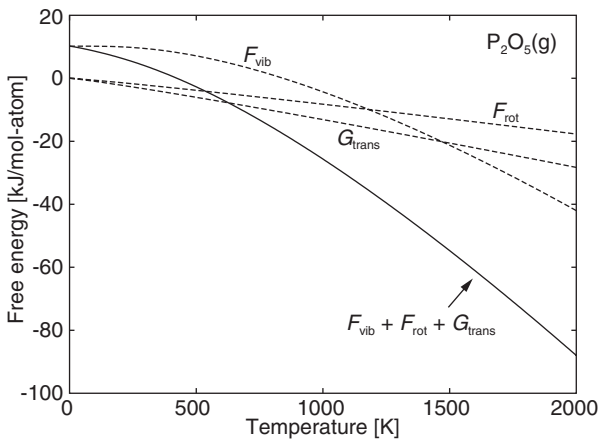

FIG. 5. The vibrational, rotational, and translational free energies of P_2O_5(g) under 1 atm (broken lines). The summation of the three contributions is also shown by the solid line.

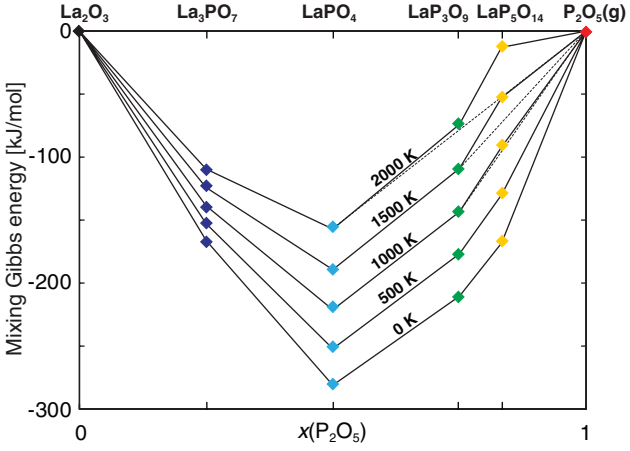

FIG. 7. (Color online) Mixing Gibbs energies under 1 atm of La_2O_3, La_3PO_7, $LaPO_4$, LaP_3O_9, LaP_5O_{14}, and P_2O_5(g) at 0, 500, 1000, 1500, and 2000 K, with reference to the two end members.

TABLE II. Mixing Gibbs energies under 1 atm in the La_2O_3-P_2O_5 system at 0, 298, 500, 1000, 1500, and 2000 K.

	Mixing Gibbs energy (kJ/mol)					
Temperature (K)	La_2O_3(s)	La_3PO_7(s)	$LaPO_4$(s)	LaP_3O_9(s)	LaP_5O_{14}(s)	P_2O_5(g)
0	0	−166	−281	−210	−168	0
298	0	−158	−264	−190	−145	0
500	0	−153	−252	−177	−130	0
1000	0	−139	−221	−143	−92	0
1500	0	−124	−189	−109	−53	0
2000	0	−110	−157	−74	−13	0

while the weak La-O bonds make the low-frequency modes. The barycenter of the whole vibrational density of states, therefore, tends to increase with increasing the P_2O_5 composition in the La_2O_3-P_2O_5 system. As will be described later, the tendency in the vibrational density of states has notable impacts on the relative Gibbs energies at finite temperatures.

C. Gibbs energies

Figure 4 shows the vibrational free energy, F_{vib}, of each phase as a function of temperature, which monotonically decreases with increasing temperature following Eq. (3). With increasing the P_2O_5 composition, $x(P_2O_5)$, the contribution of the zero-point vibrational energies increases, while the temperature dependence of F_{vib} decreases in this temperature range. These tendencies reflect the fact that the ratio of the high-frequency vibrational modes increases with increasing $x(P_2O_5)$. It is interesting that the vibrational free energy of La_3PO_7 coincide with the average line of La_2O_3 and $LaPO_4$ (dotted line), resulting from the averaged vibrational spectra of the two phases as a crude approximation.

As for P_2O_5(g), the rotational and translational free energies should be also taken into account. Figure 5 shows the three contributions to the Gibbs energy by the vibrations, rotations, and translations under 1 atm. The contributions of the rotations and the translations result in large temperature dependence of the total Gibbs energy. Note that P_2O_5 gas has a unique feature in the Gibbs energy compared with gas phases composed of simple molecules, such as N_2 and O_2. In such simple molecules, the rotational and translational contributions are much larger than the vibrational contributions, because they have only a few vibrational modes per molecule. For example, diatomic molecules have only one stretching mode. However, P_2O_5 gas (P_4O_{10} molecules consisting of 14 atoms) has 36 vibrational modes, leading to the large vibrational free energies comparable to the other two contributions.

The temperature dependences of the standard Gibbs energies are available only for La_2O_3, $LaPO_4$, and P_2O_5(g) in the literature.[31–33] Figure 6 is the comparison of the temperature dependences between the calculated and reported standard Gibbs energies. Our calculated values (solid lines) are in reasonable agreement with the available data (broken lines). For instance, the differences between the calculated and reported values at 1500 K are 1.8 kJ/mol-atom (19 meV/atom) for La_2O_3, 0.02 kJ/mol-atom (0.2 meV/atom) for $LaPO_4$, and 1.7 kJ/mol-atom (18 meV/atom) for P_2O_5(g).

D. Phase stabilities

It is now possible to discuss the phase stabilities in the La_2O_3-P_2O_5 system using the calculated Gibbs energies, which have not been reported so far except those of La_2O_3, $LaPO_4$, and P_2O_5(g). Figure 7 shows the mixing Gibbs energies under 1 atm for La_3PO_7, $LaPO_4$, LaP_3O_9, and LaP_5O_{14} at several temperatures from 0 to 2000 K. The solid polygonal lines in the figure connect all the compounds at each temperature. The dotted polygonal lines show the convex hull of the free energy. For the readers' convenience, the calculated values of the mixing Gibbs energies are listed in Table II.

With increasing temperature, stability of high $x(P_2O_5)$ phases, i.e., LaP_3O_9 and LaP_5O_{14}, decreases. The behavior is most clearly seen for LaP_5O_{14} in which the relative Gibbs energy is much higher than the value on the convex hull. The instability can be ascribed to the larger temperature dependence of the free energy of P_2O_5(g) compared to the crystalline phases. According to the calculated Gibbs energies, the following decomposition reactions of LaP_3O_9 and LaP_5O_{14} proceed

$$LaP_3O_9 \rightarrow LaPO_4 + P_2O_5(g), \quad (4)$$

$$LaP_5O_{14} \rightarrow LaP_3O_9 + P_2O_5(g). \quad (5)$$

The calculated equilibrium P_2O_5(g) partial pressures reach the atmospheric pressure at 1880 and 890 K, respectively. On the other hand, the "gradual" pyrolyses of LaP_3O_9 and LaP_5O_{14} have been experimentally observed at 1073 K[34] and 973 K,[35] respectively. The stability of LaP_5O_{14} seems to be underestimated in the present study, since its large instability by our calculations at the reported temperature.

IV. CONCLUSIONS

Phase stabilities in the La_2O_3-P_2O_5 pseudobinary system at finite temperatures were theoretically analyzed from first principles. The Gibbs energies of six compounds, i.e., La_2O_3, La_3PO_7, $LaPO_4$, LaP_3O_9, LaP_5O_{14}, and P_2O_5(g) were calculated as a function of temperature. Dynamical contributions, i.e., vibrations, rotations, and translations, were taken into account for their Gibbs energy calculations. The vibrational spectra strongly reflect the crystal structures and bonding states. The strong covalent P-O bonds in the PO_4 units and the relatively weak La-O bonds determine the vibrational states. In La_3PO_7 with a stacked structure of La_2O_3-like and $LaPO_4$-like layers, the vibrational spectrum is approximately

the average of the two phases, resulting in the average vibrational free energy. On the other hand, the P_2O_5-rich compounds, i.e., LaP_3O_9 and LaP_5O_{14}, cannot be treated in the same manner. Their PO_4 units form corner-sharing networks whose vibrations are strongly correlated. The networks raise the vibrational frequencies, leading to high-frequency modes up to 40 THz. The calculated Gibbs energies of La_2O_3, $LaPO_4$, and P_2O_5(g) were found to differ from the experimental values by less than 2kJ/mol-atom (20 meV/atom) at 1500 K. The Gibbs energies and the phase stabilities of the other three compounds, La_3PO_7, LaP_3O_9, and LaP_5O_{14}, yet unknown so far, have been evaluated.

ACKNOWLEDGMENT

This study was supported by the Elements Science and Technology Project from the Ministry of Education, Culture, Sports, Science, and Technology (MEXT) of Japan.

*Corresponding author: k.toyoura0315@gmail.com

[1] Y. Takita, K. Sano, T. Muraya, H. Nishiguchi, N. Kawata, M. Ito, T. Akbay, and T. Ishihara, Appl. Catal. A **170**, 23 (1998).
[2] U. Rambabu and S. Buddhudu, Opt. Mater. **17**, 401 (2001).
[3] N. Kitamura, K. Amezawa, Y. Tomii, and N. Yamamoto, Solid State Ionics **162**, 161 (2003).
[4] M. W. Chase Jr., *NIST-JANAF Thermochemical Tables*, 4th ed, Monograph No. 9 (The American Chemical Society and American Institute of Physics, New York, 1998).
[5] I. Barin and G. Platzki, *Thermochemical Data of Pure Substances*, 3rd ed. (VCH, Weinheim, New York, 1995).
[6] H. D. Park and E. R. Kreidler, J. Am. Ceram. Soc. **67**, 23 (1984).
[7] J. Kropiwnicka and T. Znamierowska, Pol. J. Chem. **62**, 587 (1988).
[8] V. H. Schäfer and V. P. Orlovskii, Z. Anorg. Allg. Chem. **390**, 13 (1972).
[9] I. A. Rat'kovskii, B. A. Butylin, G. I. Novikov, V. P. Orlovskii, and E. A. Ionkina, Dokl. Chem. **210**, 428 (1973).
[10] D. Usubaliev, Russ. J. Phys. Chem. **49**, 943 (1975).
[11] L. A. Marinova and V. N. Yaglov, Russ. J. Phys. Chem. **50**, 477 (1976).
[12] V. P. Orlovskii, T. V. Belyaevskaya, and V. I. Bugakov, Russ. J. Phys. Chem. **22**, 1272 (1977).
[13] S. V. Ushakov, K. B. Helean, and A. Navrotsky, J. Mater. Res. **16**, 2623 (2001).
[14] C. Thiriet, R. J. M. Konings, P. Javorský, N. Magnani, and F. Wastin, J. Chem. Thermodyn. **37**, 131 (2005).
[15] E. N. Silva, A. P. Ayala, I. Guedes, C. W. A. Paschoal, R. L. Moreira, C. K. Loong, and L. A. Boatner, Opt. Mater. **29**, 224 (2006).
[16] P. E. Blöchl, Phys. Rev. B **50**, 17953 (1994).
[17] G. Kresse and J. Hafner, Phys. Rev. B **47**, RC558 (1993).
[18] G. Kresse and J. Hafner, Phys. Rev. B **48**, 13115 (1993).
[19] G. Kresse and J. Hafner, Phys. Rev. B **49**, 14251 (1994).
[20] G. Kresse and J. Furthmuller, Comput. Mater. Sci. **6**, 15 (1996).
[21] G. Kresse and J. Furthmuller, Phys. Rev. B **54**, 11169 (1996).
[22] J. P. Perdew, K. Burke, and M. Ernzerhof, Phys. Rev. Lett. **77**, 3865 (1996).
[23] K. Parlinski, Z.-Q. Li, and Y. Kawazoe, Phys. Rev. Lett. **78**, 4063 (1997).
[24] A. Togo, F. Oba, and I. Tanaka, Phys. Rev. B **78**, 134106 (2008).
[25] W. C. Koehler and E. O. Wollan, Acta Crystallogr. **6**, 741 (1953).
[26] E. G. Tselebrovskaya, B. F. Dzhurinskii, and O. I. Lyamina, Inorg. Mater. **33**, 52 (1997).
[27] Y. Ni, J. M. Hughes, and A. N. Mariano, Am. Mineral. **80**, 21 (1995).
[28] J. Matuszewski, J. Kropiwnicka, and T. Znamierowska, J. Solid State Chem. **75**, 285 (1988).
[29] J. M. Cole, M. R. Lees, J. A. K. Howard, R. J. Newport, G. A. Saunders, and E. Schönherr, J. Solid State Chem. **150**, 377 (2000).
[30] K. K. Palkina, N. E. Kuz'mina, B. F. Dzhurinskii, and E. G. Tselebrovskaya, Dokl. Chem. **341**, 127 (1995).
[31] I. Barin, *Thermochemical Data of Pure Substances*, 3rd ed. (VCH Verlagsgesellschaft mbH, Weinheim, 1995), p. 936.
[32] K. Popa, D. Sedmidubsky, O. Benes, C. Thiriet, and R. Konings, J. Chem. Thermodyn. **38**, 825 (2006).
[33] I. Barin, *Thermochemical Data of Pure Substances*, 3rd ed. (VCH Verlagsgesellschaft mbH, Weinheim, 1995), p. 1265.
[34] K. Amezawa, Y. Kitajima, Y. Tomii, and N. Yamamoto, Electrochem. Solid State Lett. **7**, 511 (2004).
[35] W. Jungowska and T. Znamierowska, Mater. Chem. Phys. **48**, 230 (1997).